Transactions, SMiRT-26
Berlin/Potsdam, Germany, July 10-15, 2022
Division IV

EMPIRICAL ASSESSMENT OF KINEMATIC SOIL-STRUCTURE INTERACTION EFFECTS FOR VERTICAL MOTIONS IN KASHIWAZAKI-KARIWA INSTRUMENTED STRUCTURES

Peiman Zogh[1], Ramin Motamed[2], and Keri Ryan[3]

[1] Graduate Research Assistant and Ph.D. Student, Department of Civil and Environmental Engineering, University of Nevada, Reno, USA
[2] Associate Professor, Department of Civil and Environmental Engineering, University of Nevada, Reno, USA (motamed@unr.edu)
[3] Professor, Department of Civil and Environmental Engineering, University of Nevada, Reno, USA

ABSTRACT

The current simplified methods for kinematic soil-structure interaction (SSI) effects are limited only to horizontal ground motions for buildings with regular foundation width and embedment depth. Therefore, there is a lack of any recommendations for vertical ground motions. Kinematic SSI is quantified in the design guidelines by the ratio between response spectra of foundation motion (FM) and free-field motion (FFM) which is called the Ratio of Response Spectra (RRS). This study presents empirical vertical translational *RRS*s based on recorded data at a well-instrumented facility in Japan for a better understanding of kinematic SSI effects on vertical ground motions. Then, a comparison between empirical vertical and simplified horizontal *RRS*s is made, illustrating the need to establish a simplified procedure for vertical translational *RRS*. The overall trends of comparisons indicate that simplified horizontal *RRS*s tend to overestimate the foundation vertical motions and empirical horizontal *RRS*s tend to underestimate them. The extent of the underestimation by empirical horizontal *RRS*s is higher than the extent of overestimation by code-based horizontal *RRS*s.

INTRODUCTION

The earthquake-induced free-field ground motion (FFM) can be affected by different factors such as earthquake source, travel path effects, and local site effects. In addition, the motion experienced by a structure can be substantially influenced by the soil-structure interaction (SSI) effects (Stewart et al., 1999). As an example, foundation motions (FM) at the structural foundation level can deviate from FFM. Two mechanisms that simultaneously occur and cause these deviations are inertial and kinematic SSI (Borghei and Ghayoomi, 2019) of which kinematic SSI is a result of stiffness of the foundation elements (Ghayoomi and Dashti, 2015; NIST, 2012).

Kinematic SSI effects can be evaluated using simplified procedures that are semi-empirical and developed from earthquake motion databases limited to regular multi-story buildings in California (Kim and Stewart, 2003; Veletsos et al., 1997; Veletsos and Meek, 1974; Veletsos and Prasad, 1989). Kinematic SSI in the design guidelines such as ASCE/SEI 41-17 (ASCE, 2017) is quantified by the ratio between acceleration response spectra of FM and FFM which is called the Ratio of Response Spectra (*RRS*).

The current kinematic SSI simplified methods are limited only to horizontal ground motions for buildings with regular foundation width and embedment depth, and there is a lack of any recommendations for vertical motions (FEMA, 2005; Zogh et al., 2021). Figure 1 demonstrates differences in foundation translational displacements in horizontal and vertical directions. As a result, there remains an important research question on the extent of kinematic SSI for vertical ground motions in buildings with large

foundations and deep embedments such as nuclear power plant (NPP) structures. In addition, adequate site-specific design procedures for vertical ground motions are required in a variety of design applications. Design procedures for vertical ground motions are important due to observations that they can exceed horizontal ground motions at distances closer to the earthquake source and at short periods of the incident earthquake waves. Furthermore, the properties of the vertical ground motions are not characterized as well as the horizontal ground motions (Beresnev et al., 2002).

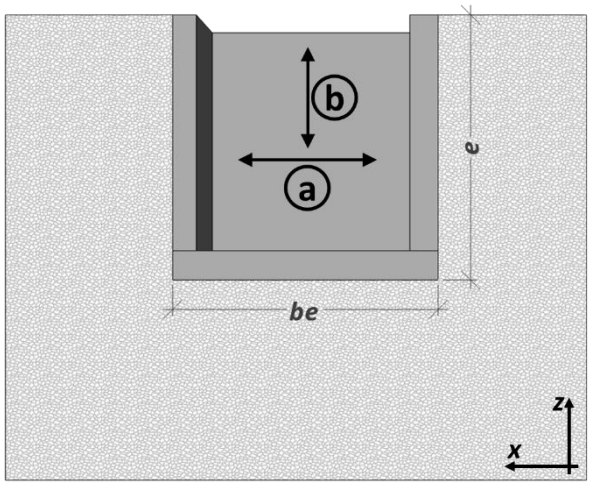

Figure 1. Foundation translational displacements: (a) horizontal, and (b) vertical.

The objective of this study is to compare empirical vertical and horizontal as well as the simplified code-based horizontal *RRS*s to evaluate the extent of deviations between them. Empirical vertical and horizontal *RRS*s are calculated based on recorded data at a well-instrumented nuclear facility in Japan. Recorded motions at multiple structures within the Kashiwazaki-Kariwa Nuclear Power Plant (KKNPP) facility are used to derive vertical and horizontal *RRS*s from multiple earthquake recordings to assess the extent of kinematic SSI in nuclear structures when subjected to multi-directional shakings including vertical and horizontal components.

KASHIWAZAKI-KARIWA (KKNPP) INSTRUMENTED SITE

This section introduces the KKNPP site and its adjacent downhole arrays properties and geotechnical sub-surface characteristics. The KKNPP site includes seven units (Fig. 2); each has a reactor and a turbine building with properties listed in Table 1. Furthermore, the details of instrumentation at one of these buildings are illustrated in Figure 3(a). A recording from a sensor at the foundation level—such as the reactor in Unit 1 (Figure 3a)—is used to represent the FM. At each unit building, a recording from a sensor near the roof elevation—shown in Figure 3(a)—is also used to empirically estimate the flexible-base first-mode frequency of the building following the Stewart and Fenves (1998) method.

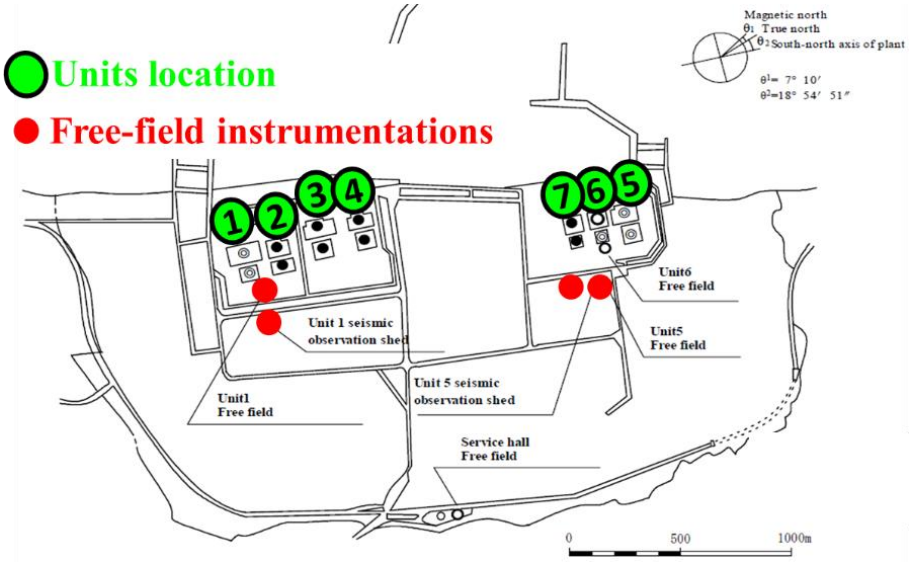

Figure 2. Buildings and free-field stations at KKNPP in Japan (original image provided by the Tokyo Electric Power Company).

In addition, the soil shear wave velocity profiles are presented in Figure 3(b) at the location of three downhole arrays. At each soil profile, the average shear wave velocity over the depth of embedment ($\overline{V_s}$) is calculated and presented in Table 1.

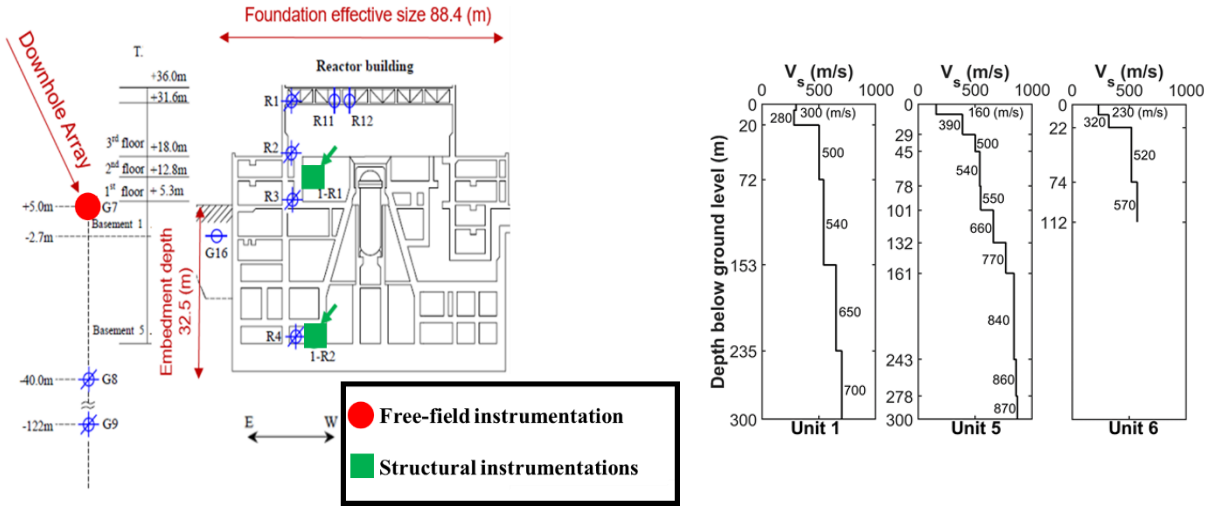

Figure 3. (a) Cross-sectional view across E-W direction and instrumentations of the building and free-field downhole array at the reactor of Unit 1 at KKNPP (original image provided by the Tokyo Electric Power Company). (b) Shear wave velocity profiles at downhole arrays at KKNPP (Unit 6 is not free-field) (Zogh et al., 2021).

Also, Table 1 presents each building's characteristics, including the total foundation area in m^2, the effective size of the foundation (b_e) in m, the embedment depth (e) in m, and the average shear wave velocity over the depth of embedment ($\overline{V_s}$) in m/s. Note that the values included in Table 1 are used in the code-based kinematic SSI equations for calculating horizontal translational *RRS*s.

Table 1: Building characteristics at the KKNPP site (Zogh et al., 2021).

Unit	Building	Building Type	*Footing area* (m^2)	b_e (m)	e (m)	$\overline{V_s}$ (m/s)
1	TU1	-	-	-	-	-
	RE1	Reactor	7832	88.4	33	342.0
2	TU2	Turbine	8611	92.8	21	293.5
	RE2	Reactor	6723	82.0	38	357.2
3	TU3	Turbine	7560	86.9	21	293.5
	RE3	Reactor	6630	81.4	38	357.2
4	TU4	Turbine	7811	88.4	21	293.5
	RE4	Reactor	6715	81.9	38	357.2
5	TU5	-	-	-	-	-
	RE5	Reactor	6560	81.0	30	263.6
6	TU6	-	-	-	-	-
	RE6	Reactor	3658	60.5	20	227.4
7	TU7	Turbine	7566	87.0	22	235.6
	RE7	Reactor	3363	58.0	20	227.4

RECORDED EARTHQUAKE DATABASE

In this study, seven seismic events are included in the dataset consisting of a mainshock and its six aftershocks of the 2007 M6.8 Niigata-ken Chuetsu-Oki earthquake. The characteristics of each event are presented in Table 2. The recorded earthquake motions are raw recordings needing to be filtered and processed. Hence, the NGA West2 project method (Boore et al., 2012) is employed to filter and process the data (Boore, 2005; Boore and Akkar, 2003; Boore and Bommer, 2005; Pilz and Parolai, 2012). In addition, as a control of the filtered recordings, a signal-to-noise ratio (SNR) analysis is conducted (SNR = 0.3 dB) that can avoid noise interference in the *RRS* calculation (Zogh et al., 2021).

Table 2: Earthquake events considered in this study.

Events	Year/Month/Day	Latitude (°)	Longitude (°)	Magnitude (M_{JMA})	Depth (km)	Distance (km)
NCO (MS)	2007/07/16	37.56	138.61	6.8	16.75	15.56
NCO (AS1)	2007/07/16	37.46	138.57	3.7	22.00	05.17
NCO (AS2)	2007/07/16	37.50	138.64	5.8	22.53	09.56
NCO (AS3)	2007/07/16	37.42	138.56	4.2	18.85	03.54
NCO (AS4)	2007/07/16	37.51	138.63	4.4	20.42	10.34
NCO (AS5)	2007/07/25	37.53	138.72	4.8	24.21	16.18
NCO (AS6)	2007/08/04	37.42	138.54	3.2	18.00	05.31
Notes: M_{jma} = Magnitude based on the Japan Meteorological Agency database, NCO(MS): mainshock of the Niigata-ken Chuetsu-Oki earthquake, NCO(AS#): aftershock of the Niigata-ken Chuetsu-Oki earthquake (Data provided by the Tokyo Electric Power Company).						

RESULTS AND DISCUSSIONS

The simplified code-based equations for horizontal translational motions (e.g. procedures included in ASCE/SEI 41-17 and ASCE/SEI 7-16) use several parameters mentioned in Table 1 (i.e. b_e, e, and $\overline{V_s}$) to estimate kinematic SSI effects in terms of *RRS*. In this study, the ASCE/SEI 41-17 procedure is used to calculate *RRS* and it is called RRS_{Code}. Note that reduced $\overline{V_s}$ values should be used for the calculation of simplified equations considering the soil site class and earthquake motion intensity. Furthermore, $\overline{V_s}$ reduction factors can relate the nonlinear behaviour of the soil to the RRS_{Code} amplitudes especially in large-magnitude events.

In addition, the filtered processed acceleration recordings are used to develop *RRS*. The empirical *RRS* for horizontal and vertical translations are calculated using the following equation:

$$RRS\,(f) = \frac{S_{a-FM}(f)}{S_{a-FFM}(f)} \tag{1}$$

where, S_{a-FM} is the acceleration response spectrum of FM in the frequency domain, S_{a-FFM} is the response spectrum of FFM in the frequency domain, and $RRS\,(f)$ is the empirical *RRS* as a function of frequency. Note that the *RRS* for horizontal and vertical motions are referred to as RRS_H and RRS_V. Figure 4 shows sample acceleration time histories of vertical FFM and FM recorded at the RE1 building of KKNPP using in the calculation of S_{a-FFM} and S_{a-FM}.

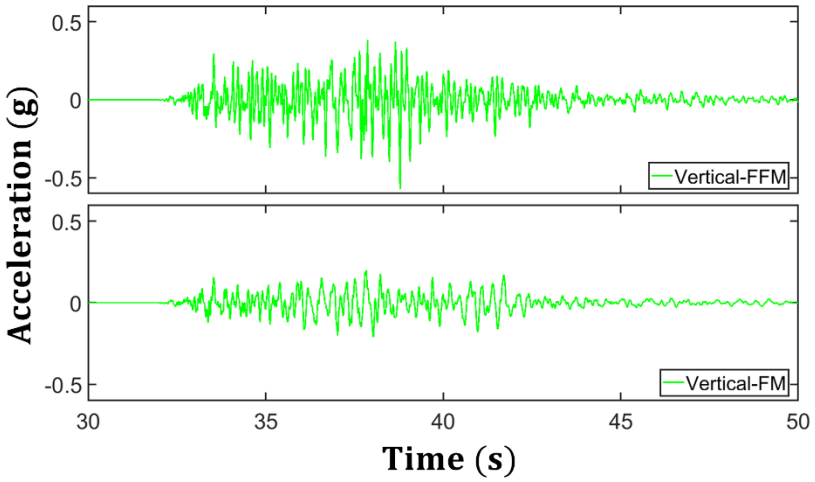

Figure 4. Recorded vertical acceleration histories FM and FFM at RE1 building of KKNPP during the NCO(MS).

Figure 5(a) compares the RRS_V with the RRS_{Code} for all available earthquake recordings at buildings of the KKNPP site alongside the corresponding mean curves. It is noteworthy that the RRS_{Code} is developed for horizontal translational motions. Note that deviations between RRS_{Code} curves are due to variable structural and soil characteristics of the buildings but the minimum value for all of them is 0.5 based on the ASCE/SEI 41-17 procedure. In addition, Figure 5(b) compares the empirical RRS_V and RRS_H alongside the mean curves. Note that there were different minimum usable frequencies for each recording based on each building's accelerometer characteristics.

In Figure 5(b), the amplitude of individual RRS_H curves and their mean tend to a constant value of around 0.25 in the frequency range of 2~3 Hz. This trend is called saturation in horizontal *RRS* amplitudes and is also reflected in Figure 5(a) for RRS_{Code} curves, although the constant in ASCE/SEI 41-17 is set to

be 0.5 (FEMA, 2005). Furthermore, a saturation in amplitudes can be also seen in RRS_V curves, with an average value around 0.25, similar to RRS_H amplitudes. On the other hand, the saturation in amplitudes of RRS_V seems to start from higher frequencies than for RRS_H (around 10 Hz). In fact, this difference can be a result of the domination of distinct types of incident waves in vertical or horizontal ground motions (P, SV, or SH waves) (Amirbekian and Bolt, 2019; Beresnev et al., 2002; Silva, 1997; Yang et al., 2002; Yang and Sato, 2000).

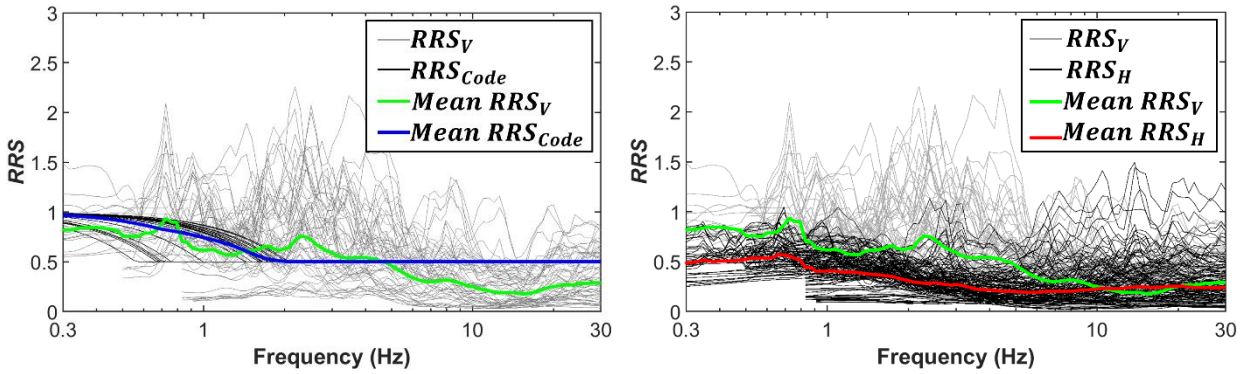

(a) (b)

Figure 5. (a) All individual and mean curves of RRS_V and RRS_{Code}, (b) all individual and mean curves of RRS_V and RRS_H.

For each pair of *RRS*s, the RRS_V and RRS_{Code} or the RRS_V and RRS_H are compared by computing residuals between them using the following equations:

.

$$R_{V-Code} = ln(RRS_V) - ln(RRS_{Code}) \quad (2)$$

$$R_{V-H} = ln(RRS_V) - ln(RRS_H) \quad (3)$$

where, R is the residual value and *ln* is the natural logarithm. Note that using logarithmic values can make differences in the results in a similar order, hence comparing the results and associated deviations becomes easier. The residual calculation can make the comparisons independent of structure and soil characteristics. Note that a positive residual indicates that the vertical FM is underestimated by using the RRS_{Code} or RRS_H whereas, a negative residual indicates that it is overestimated.

Figures 6(a) and (b) present all the individual residuals along with the mean curves for both the R_{V-Code} and R_{V-H}. Based on the mean values for R_{V-Code} for frequency ranges lower than around 5 Hz, the residual values seem to be negligible indicating a good match between RRS_V and RRS_{Code}, whereas at higher frequencies, the RRS_{Code} overestimates the vertical response (Figure 6a). The overestimation at the higher frequencies can be attributed to the type of dominated incident waves in vertical earthquake motions. It was shown by Beresnev et al. (2002) that the vertical earthquake motions are dominated by shear waves (SV-waves) at frequency ranges up to approximately 10 Hz, above which the contribution of compressional waves (P-waves) is greater.

On the other hand, different behaviour is observed in Figure 6(b) showing that generally, the empirical horizontal *RRS* amplitudes are less than the empirical vertical *RRS* amplitudes across the frequency domain. Note that this trend is diminished at frequencies larger than 10 Hz.

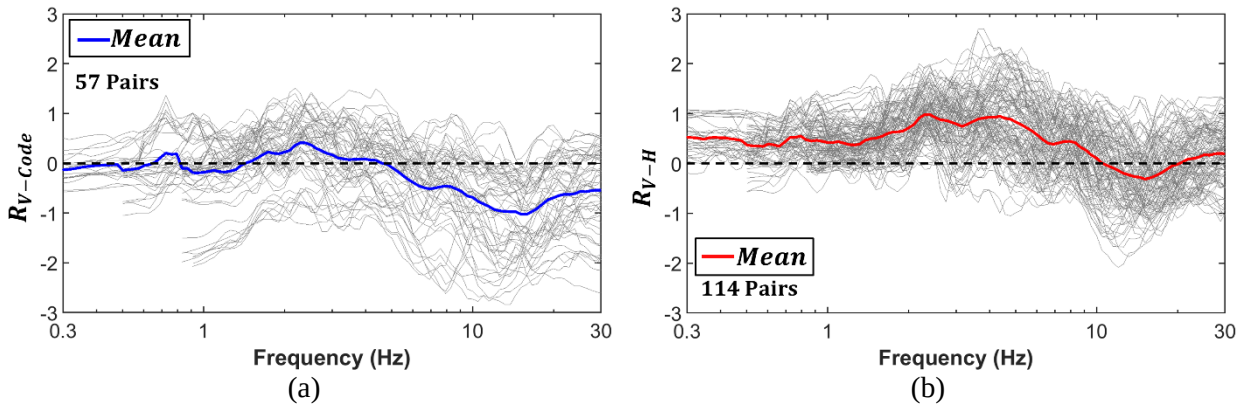

Figure 6. (a) All individual and mean residual curves of R_{V-Code}, (b) all individual and mean residual curves of R_{V-H}.

Figure 7 compares the mean values of R_{V-Code} and R_{V-H}, and the zero residual is shown as a black dashed line. Generally, R_{V-Code} is zero or negative and R_{V-H} is positive over almost the whole frequency bandwidth. Differences between mean values of R_{V-Code} and R_{V-H} can be attributed to factors such as inertial effects that are included in a narrow-banded frequency range of empirical horizontal *RRS*s but not included in simplified code-based procedures for calculating *RRS*s.

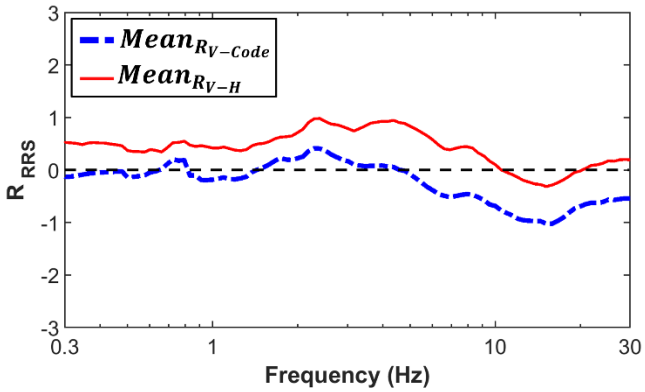

Figure 7. Mean values of R_{RRS}.

CONCLUSIONS

In this study, the extent of kinematic SSI effects for vertical ground motions was assessed at the KKNPP site based on the recorded ground motions at this site in Japan (57 vertical motion recordings and 114 horizontal motion recordings in both EW and NS directions). The results were then compared in the form of residuals to each other and to the simplified code-based equations. The simplified code-based equations were defined for estimating horizontal translational motions. The conclusions of this study are as follows:

- The overall trends of comparisons indicate that simplified code-based horizontal *RRS*s tend to match with or overestimate the foundation vertical motions and empirical horizontal *RRS*s tend to underestimate them.
- The extent of the underestimation by empirical horizontal *RRS*s is at a wider frequency bandwidth compared to the extent of overestimation by simplified code-based horizontal *RRS*s and this difference can be attributed to the inertial effects.

- The RRS_V values are around a constant number after frequencies around 10 Hz that the saturation of *RRS* amplitudes occurred. Whereas, RRS_H values are constant after the frequency range of 2~3 Hz. In addition, both of these constant values are 0.25 on average. Note that the constant value in RRS_{Code} is 0.5 based on ASCE/SEI 41-17 but occurs at the same frequency range as RRS_H.
- The differences between horizontal and vertical *RRS*s can be due to the domination of different types of earthquake incident waves in horizontal and vertical foundation translations (compression or shear waves).
- Results of this study suggest the need for future research to establish a dedicated semi-empirical simplified procedure for estimating foundation vertical earthquake motions.

ACKNOWLEDGEMENTS

This work is funded by the Nuclear Safety Research and Development (NSR&D) Program, which is managed by the Office of Nuclear Safety within the Office of Environment, Health, Safety, and Security (AU) to provide corporate-level leadership supporting nuclear safety research and development throughout the Department of Energy (DOE). The authors would like to thank Patrick Frias the NSR&D Program manager. Michael Salmon and Richard Lee, our collaborators at Los Alamos National Laboratory (LANL), provided valuable input during this work, which is greatly acknowledged. The authors also acknowledge that the ground motion data used in this study belong to Tokyo Electric Power Company and the distribution license of the data belongs to the Japan Association for Earthquake Engineering.

REFERENCES

American Society of Civil Engineers. (2016). *ASCE/SEI 7-16 (Minimum design loads and associated criteria for buildings and other structures)*. https://doi.org/10.1061/9780784414248

American Society of Civil Engineers. (2017). *ASCE/SEI 41-17 (Seismic evaluation and retrofit of existing buildings)*. https://doi.org/10.1061/9780784414859

Amirbekian, R. V., & Bolt, B. A. (2019). "Spectral comparison of vertical and horizontal seismic strong ground motions in alluvial basins," 14(4), 573–595. https://doi.org/10.1193/1.1586017

Beresnev, I. A., Nightengale, A. M., & Silva, W. J. (2002). "Properties of vertical ground motions," *Bulletin of the Seismological Society of America*, *92*(8), 3152–3164. https://doi.org/10.1785/0120020009

Boore, D. M. (2005). "On pads and filters: processing strong-motion data," *Bulletin of the Seismological Society of America*, 95(2), 745–750. https://doi.org/10.1785/0120040160

Boore, D. M., & Akkar, S. (2003). "Effect of causal and acausal filters on elastic and inelastic response spectra," *Earthquake Engineering & Structural Dynamics*, 32(11), 1729–1748. https://doi.org/10.1002/eqe.299

Boore, D. M., & Bommer, J. J. (2005). "Processing of strong-motion accelerograms: Needs, options and consequences," *Soil Dynamics and Earthquake Engineering*, 25(2), 93–115. https://doi.org/10.1016/j.soildyn.2004.10.007

Boore, D. M., Sisi, A. A., & Akkar, S. (2012). "Using pad-stripped acausally filtered strong-motion data," *Bulletin of the Seismological Society of America*, 102(2), 751–760. https://doi.org/10.1785/0120110222

Borghei, A., & Ghayoomi, M. (2019). "The role of kinematic interaction on measured seismic response of soil-foundation-structure systems," *Soil Dynamics and Earthquake Engineering*, 125, 105674. https://doi.org/10.1016/j.soildyn.2019.05.013

Federal Emergency Management Agency (FEMA). (2005). "Recommended provisions for improvement of nonlinear static seismic analysis procedures," *FEMA 440*, Washington D.C., Washington D.C.

Ghayoomi, M., & Dashti, S. (2015). "Effect of Ground Motion Characteristics on Seismic Soil-Foundation-Structure Interaction," *Meridian.Allenpress.Com*, 31(3), 1789–1812. https://doi.org/10.1193/040413EQS089M

Givens, M., Mikami, A., Kashima, T., & Stewart, J. (2012). "Kinematic soil-structure interaction effects

from building and free-field seismic arrays in Japan," *9th International Conference on Urban Earthquake Engineering/ 4th Asia Conference on Earthquake Engineering*. https://escholarship.org/uc/item/8mk017th

Kim, S., & Stewart, J. P. (2003). "Kinematic soil-structure interaction from strong motion recordings," *Journal of Geotechnical and Geoenvironmental Engineering*, 129(4), 323–335. https://doi.org/10.1061/(ASCE)1090-0241(2003)129:4(323)

Li, G., Motamed, R., & Dickenson, S. (2018). "Evaluation of one-dimensional multi-directional site response analyses using geotechnical downhole array data in California and Japan," *Earthquake Spectra*, 34(1), 349–376. https://doi.org/10.1193/010617EQS005M

NIST. (2012). *Soil-structure-interaction for building structures (NIST GCR 12-917-21)*.

Pilz, M., & Parolai, S. (2012). "Tapering of windowed time series," In *New Manual of Seismological Observatory Practice 2 (NMSOP-2)* (pp. 1–4). https://doi.org/10.2312/GFZ.NMSOP-2_IS_14.1

Silva, W. (1997). "Characteristics of vertical strong ground motions for applications to engineering design," In *Proc. Of theFHWA/NCEER Workshop on the Nat'l Representation of Seismic Ground Motion for New and Existing Highway Facilities*.

Stewart, J. P., & Fenves, G. L. (1998). "System identification for evaluating soil-structure interaction effects in buildings from strong motion recordings," *Earthquake Engineering and Structural Dynamics*, 27(8), 869–885. https://doi.org/10.1002/(SICI)1096-9845(199808)27:8<869::AID-EQE762>3.0.CO;2-9

Stewart, J. P., Fenves, G. L., & Seed, R. B. (1999). "Seismic soil-structure interaction in buildings. I: Analytical methods," *Journal of Geotechnical and Geoenvironmental Engineering*, 125(1), 26–37. https://doi.org/10.1061/(ASCE)1090-0241(1999)125:1(26)

Veletsos, A., & Meek, J. (1974). "Dynamic behaviour of building-foundation systems," *Earthquake Engineering & Structural Dynamics*, 121–138. https://doi.org/10.1002/eqe.4290030203

Veletsos, A., & Prasad, A. (1989). "Seismic Interaction of Structures and Soils: Stochastic Approach," *Journal of Structural Engineering*, 115(4), 935–956. https://doi.org/10.1061/(ASCE)0733-9445(1989)115:4(935)

Veletsos, A., Prasad, A., & Wu, W. (1997). "Transfer functions for rigid rectangular foundations," *Earthquake Engineering & Structural Dynamics*, 26(1), 5–17. https://doi.org/10.1002/(SICI)1096-9845(199701)26:1<5::AID-EQE619>3.0.CO;2-X

Yang, J., & Sato, T. (2000). "Interpretation of seismic vertical amplification observed at an array site," *Bulletin of the Seismological Society of America*, 90(2), 275–285. https://doi.org/10.1785/0119990068

Yang, J., Sato, T., Savidis, S., & Li, X. S. (2002). "Horizontal and vertical components of earthquake ground motions at liquefiable sites," *Soil Dynamics and Earthquake Engineering*, 22(3), 229–240. https://doi.org/10.1016/S0267-7261(02)00010-6

Zogh, P., Motamed, R., & Ryan, K. (2021). "Empirical evaluation of kinematic soil-structure interaction effects in structures with large footprints and embedment depths," *Soil Dynamics and Earthquake Engineering*, 149, 106893. https://doi.org/10.1016/J.SOILDYN.2021.106893